A Site-Specific ESR Spin-Labeling Study of Molecular Motion in Microphase-Separated Polystyrene-*block*-poly(methyl acrylate) with Lamellar Morphology

Yohei Miwa,[†] Katsuhiro Yamamoto,[†] Masato Sakaguchi,[‡] Masahiro Sakai,[§] Kenichi Tanida,[†] Shigeo Hara,[†] Shigeru Okamoto,[†] and Shigetaka Shimada*[,†]

Department of Materials Science & Engineering, Nagoya Institute of Technology, Gokiso-cho, Showa-ku, Nagoya 466-8555, Japan; Nagoya Keizai University, 61 Uchikubo, Inuyama 484-8503, Japan; and Research Center for Molecular-Scale Nanoscience, Institute for Molecular Science, 38 Nishigo-Naka, Myodaiji, Okazaki 444-8585, Japan

Received July 28, 2003; Revised Manuscript Received November 6, 2003

ABSTRACT: Molecular motion at the specific sites of polystyrene-*block*-poly(methyl acrylate) (PS-*block*-PMA) forming a lamellar morphology was studied by electron spin resonance (ESR). PS-*block*-PMA's having nearly the same molecular weight and composition were selectively spin-labeled with stable nitroxide radicals at different specific sites (each free end, inside segments of each block, or the chemical junction point between the blocks). The molecular motion was analyzed from temperature-dependent ESR spectra of the spin-labels. Enhancement of molecular mobility of the chain end in comparison with that of the inside was detected. The enhanced molecular mobility of the both ends of the PS-*block*-PMA was more remarkable than those of the both homopolymers. This was brought from the much large free volume around the chain ends of the PS-*block*-PMA because of the local high concentration of the chain ends in the lamellar microdomains. The molecular mobilities of the PS-*block*-PMA and polystyrene-*block*-poly(ethyl acrylate) (PS-*block*-PEA) labeled at the junction points were related to thermal behavior and local environment of polymer chains in the interfacial region of the lamellar microdomains. This demonstrated that the structure in the interface was heterogeneous, although the both components were mixing compatibly in the interfacial region.

Introduction

Heterogeneous block copolymers composed of blocks with significantly different glass transitions are interesting thermoplastic elastomers and have been widely studied in academic[1] and industrial[2] research on account of their unique physical and technical properties. For better understanding of these systems, a comparison of chain dynamics of the components of block copolymers with that of homopolymers is particularly informative. From this view, many authors studied glass transition temperatures (T_g) of block copolymers forming the microphase-separated structure using differential scanning calorimetry (DSC),[3−7] dynamic mechanical measurement,[8−12] dilatometry,[13] refractive index,[14] nuclear magnetic resonance (NMR),[3,15−18] and electron spin resonance (ESR).[19−22] In particular, it is well-known that the ESR with the spin-label method is one of the most advantageous methods to study the structure and dynamics behavior of polymer chains at a particular site or in a particular region.[23−31] Recently, we studied the partial molecular mobility of PS homopolymer using the selective spin-label method.[32] The molecular mobility of the chain end was compared with that of the inside of the PS chain at the α relaxation. It was revealed that the chain end has higher molecular mobility than that of the inside of the chain due to the large specific free volume around the chain end. Moreover, the molecular mobility of the chain end was enhanced with a decrease in the molecular weight. The more remarkable enhancement was caused by the much large free volume around the chain end induced by the encounter of more than two chain ends. In the present paper, the molecular motion at the specific sites of the PS-*block*-PMA forming the microphase-separated lamellar morphology was investigated. Each PS-*block*-PMA specimen was selectively spin-labeled with stable nitroxide radicals at the chain end or the inside site of the each component or the chemical junction point between the two blocks. The valuable studies for the localization of the chain ends and the chemical junction points of diblock copolymers forming the lamellar morphology were carried out by Russell et al.[33] and Matsushita et al.[34,35] utilizing small-angle neutron scattering (SANS). They revealed that the part of the block chain near the junction was strongly localized near the lamellar interface, while the chain ends were concentrated around the center of lamellar microdomains with a fairly wide distribution. It is very important to characterize the molecular mobility at the respective sites of the PS-*block*-PMA, which reflects the chain conformation and local environment in the microdomains. In particular, the spin-labels at the junction points of the PS-*block*-PMA's concentrate in the lamellar interface and the molecular motion of the spin-labels reflect characteristics of the interfacial region.

Experimental Section

Material. Styrene (ST, Extra Pure Reagent, Nacalai Tesque Co., Ltd.), methyl acrylate (MA, Extra Pure Reagent, Nacalai Tesque), *tert*-butyl acrylate (*t*BA, Extra Pure Reagent, Tokyo Chemical Co., Ltd.), ethyl acrylate (EA, Extra Pure Reagent, Nacalai Tesque), and toluene (Extra Pure Reagent, Nacalai Tesque) were distilled under reduced pressure. *N*,*N*,*N*′,*N*′,*N*″-Pentamethyldiethylenetriamine (PMDETA, 99%, Aldrich

[†] Nagoya Institute of Technology.
[‡] Nagoya Keizai University.
[§] Institute for Molecular Science.
* To whom correspondence should be addressed.

10.1021/ma035088q CCC: $27.50
Published on Web 01/03/2004

Table 1. Molecular Characteristics and $T_{5.0mT}$'s of PS, PMA, and PS-*block*-PMA

no.	sample	spin-label site	M_n[a] ($\times 10^{-3}$)	M_w/M_n[a]	$M_{n,PS}$[a] ($\times 10^{-3}$)	ϕ_{PMA}[b]	morphology[c]	spectral component[d]	$T_{5.0mT}$[d] (K)
1	PS	PS end	32	1.15	32	0		single	423
2	PS	PS inside	31	1.12	31	0		single	431
3	PS-*block*-PMA	PS end	68	1.35	27	55	lamella	two	414
4	PS-*block*-PMA	PS inside	68	1.36	28	54	lamella	two	428
5	PS-*block*-PMA	junction	56	1.19	30	51	lamella	two	398
6	PS-*block*-PMA	PMA inside	48	1.19	30	50	lamella	two	395
7	PS-*block*-PMA	PMA end	49	1.21	30	48	lamella	two	380
8	PMA	PMA end	31	1.14		100		single	363
9	PMA	PMA inside	29	1.06		100		single	367

[a] Determined by GPC with PS standards. [b] Determined by ^{1}H NMR. [c] Determined by SAXS at room temperature. [d] Determined by ESR.

Table 2. MDSC Results of Samples. Numbers Correspond to Those in Table 1

no.	sample	$T_{g,1}$ (K)	$\Delta C_{p,1}$ (J K^{-1} g^{-1})	$T_{g,PMA}$ (K)	$\Delta C_{p,PMA}$ (J K^{-1} g^{-1})	$T_{g,2}$ (K)	$\Delta C_{p,2}$ (J K^{-1} g^{-1})	$T_{g,PS}$ (K)	$\Delta C_{p,PS}$ (J K^{-1} g^{-1})
2	PS							370	0.24
5	PS-*block*-PMA	285	0.33			367	0.20		
9	PMA			284	0.35				

Table 3. Molecular Characteristics and $T_{5.0mT}$'s of Random Copolymers

sample	spin label site	M_n[a] ($\times 10^{-3}$)	M_w/M_n[a]	$M_{n,PS}$[a] ($\times 10^{-3}$)	ω_{PS}[b]	$T_{5.0mT}$[c] (K)
PS	inside	31	1.12	31	1	431
PS-*block*-PMA	junction	56	1.19	30	0.51	398
poly(ST-*random*-MA)	inside	23	1.30		0.86	426
poly(ST-*random*-MA)	inside	22	1.24		0.81	415
poly(ST-*random*-MA)	inside	31	1.27		0.67	407
poly(ST-*random*-MA)	inside	21	1.40		0.49	395
poly(ST-*random*-MA)	inside	25	1.21		0.27	380
poly(ST-*random*-MA)	inside	23	1.30		0.86	370
PMA	inside	29	1.06			367
PS-*block*-PEA	junction	60	1.10	26.1	0.45	379
poly(ST-*random*-EA)	inside	18	1.08		0.85	411
poly(ST-*random*-EA)	inside	14	1.14		0.62	395
poly(ST-*random*-EA)	inside	15	1.35		0.42	379
PEA	inside	30	1.09			326

[a] Determined by GPC with PS standards. [b] Determined by ^{1}H NMR. [c] Determined by ESR.

Chemical Co., Ltd.), 1-phenylethyl bromide (1-PEBr, 95%, Tokyo Chemical), methyl 2-bromopropionate (MBrP, 98%, Aldrich), 2-bromopropionic acid *tert*-butyl ester (2-BABE, 97%, Tokyo Chemical), CuBr (98%, Aldrich), and 2,2,6,6-tetramethyl-4-aminopiperidine-1-oxyl (4-amino-TEMPO, 99%, Aldrich) were used as received. Cyclohexane, tetrahydrofuran (THF), and methanol were obtained from Nacalai Tesque Co., Ltd. (Extra Pure Reagent) and used without further purification.

Sample Preparation and Selective Spin-Labeling. PS-*block*-PMA, poly(styrene-*random*-methyl acrylate) (poly(ST-*random*-MA)), polystyrene-*block*-poly(ethyl acrylate) (PS-*block*-PEA), poly(styrene-*random*-ethyl acrylate) (poly(ST-*random*-EA)), and PS, PMA, and PEA homopolymers were synthesized by atom transfer radical polymerization (ATRP) under reduced pressure.[36,37] The characteristics of the PS-*block*-PMA and the PS and PMA homopolymers are listed in Table 1, and those of the poly(ST-*random*-MA), PS-*block*-PEA, poly(ST-*random*-EA), and EA homopolymer are listed in Table 3. The PS and PMA homopolymers were selectively spin-labeled at the end or the inside of the chain. The selective spin-label to the chain end or the inside of each component or the chemical junction point of the PS-*block*-PMA between the PS and PMA blocks was carried out as following procedures.

1. Junction Point (5 in Figure 1). As a first component, PS was polymerized at 383 K using the CuBr/PMDETA complex and 1-PEBr as an initiator. After the polymerization, the PS was purified by the precipitation from toluene solution into excess methanol. The PS was dried in a vacuum at 323 K for 24 h. Gel permeation chromatography (GPC) determined the number-average molecular weight (M_n) and its distribution (M_w/M_n) to be 30K and 1.08, respectively. *t*BA was incorporated to the ω end of the isolated PS via the ATRP technique at 368 K with the following condition: $[PS]_0 = [tBA]_0 = 2[CuBr]_0 = 2[PMDETA]_0$ in toluene. The resultant polymer was purified by the same procedure with the PS. Nuclear magnetic resonance (NMR) revealed the attachment of the *t*BA to the ω end of the PS. The yield of the *t*BA attached at one chain end of the PS was calculated using the M_n of the PS determined by the GPC and the ratio of protons (NMR) of a *tert*-butyl group of the *t*BA to that of a benzene ring of the PS. It was confirmed that the yield of the *t*BA was 0.3 for a PS chain. This polymer was chain-extended with PMA via the ATRP at 368 K using the CuBr and PMDETA. After the extension, the reaction mixture was purified by the precipitation from toluene solution into excess methanol. After sufficient dry, the resultant polymer was washed with cyclohexane at 308 K in order to remove unreacted PS prepolymer. As a sequence, PS-*block*-PMA which had the *t*BA at the junction point was obtained. The selective spin-label at the junction point of the PS-*block*-PMA was carried out via ester−amide interchange reaction between the incorporated *tert*-butyl moiety and 4-amino-TEMPO in toluene at 283 K for 4 days. The spin-labeled PS-*block*-PMA was precipitated from a toluene/THF solution into a water/methanol mixture and filtered to remove the large amount of unreacted 4-amino-TEMPO and dried in a vacuum at 353 K for 24 h. The purification was repeated more than 4 times to completely remove the unreacted 4-amino-TEMPO.

2. Inside of PMA Block (6 in Figure 1). The isolated PS (M_n = 30K, M_w/M_n = 1.08) which had bromine at the ω end was used as a prepolymer. The isolated PS was chain-extended with PMA randomly containing a few molar percent of *t*BA. The random copolymerization of MA with *t*BA was carried out by the ATRP at 368 K with following condition: $[MA]_0 = 99[tBA]_0$, $[PS]_0 = 2[CuBr]_0 = 2[PMDETA]_0$. The PS-*block*-poly(MA-*random*-*t*BA) was purified by the precipitation from

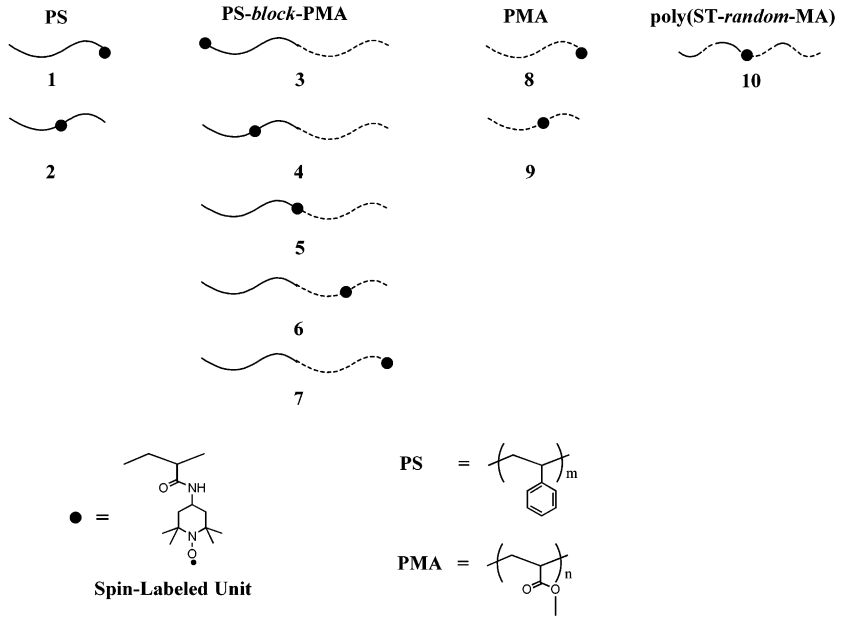

Figure 1. Chemical structures and illustrations of selectively spin-labeled PS-*block*-PMA, poly(S-*random*-MA), and PS and PMA homopolymers.

toluene solution into excess methanol. The PS-*block*-poly(MA-*random*-*t*BA) was washed with cyclohexane to remove unreacted PS prepolymer. The incorporated *tert*-butyl moieties in the PMA blocks were reacted with 4-amino-TEMPO.

3. Chain End of PMA Block (7 in Figure 1). The isolated PS (M_n = 30K, M_w/M_n = 1.08) which had bromine at the ω end was chain-extended with PMA via the ATRP. The PS-*block*-PMA was purified by the precipitation from toluene solution into excess methanol and washed with cyclohexane. The *t*BA was incorporated to the ω end of the PMA block of the isolated PS-*block*-PMA via the ATRP at 368 K with the following condition: $[PS\text{-}block\text{-}PMA]_0 = [tBA]_0 = 2[CuBr]_0 = 2[PMDETA]_0$ in toluene. The incorporated *tert*-butyl moiety at the ω end of the PMA block of the PS-*block*-PMA was reacted with 4-amino-TEMPO.

4. Inside of PS Block (4 in Figure 1). PS which was randomly containing a few molar percent of *t*BA was obtained by a random copolymerization of ST and *t*BA using the ATRP technique.[38] The poly(ST-*random*-*t*BA) was characterized by the NMR and the molar composition of ST:*t*BA = 98:2. The poly(ST-*random*-*t*BA) was chain-extended with PMA via the ATRP at 368 K using the CuBr/PMDETA complex. The poly(ST-*random*-*t*BA)-*block*-PMA was washed with cyclohexane in order to remove unreacted poly(ST-*random*-*t*BA). The incorporated *tert*-butyl moieties in the poly(ST-*random*-*t*BA)-*block*-PMA were reacted with 4-amino-TEMPO. As a result, the PS-*block*-PMA spin-labeled at the inside of the PS block was obtained.

5. Chain End of PS Block (3 in Figure 1). As a first component, PS was polymerized at 383 K via the ATRP with the CuBr/PMDETA complex and 2-BABE as an initiator. The M_n and M_w/M_n of the PS were determined by the GPC calibrated with PS standards. The isolated PS (M_n = 27 K, M_w/M_n = 1.15) was chain-extended with PMA via the ATRP. Unreacted PS prepolymers were removed from the PS-*block*-PMA through washing with cyclohexane. 4-amino-TEMPO was reacted with the incorporated *tert*-butyl moiety at the α end of the PS block in the PS-*block*-PMA.

6. Inside of Poly(ST-*random*-MA) (10 in Figure 1). The poly(ST-*random*-MA) which was randomly containing a few molar percent of *t*BA was polymerized by the ATRP with the CuBr/PMDETA complex and 1-PEBr as an initiator at 383 K with following condition: $[ST]_0 + [MA]_0 = 99[tBA]_0$, $[1\text{-}PEBr]_0 = [CuBr]_0 = [PMDETA]_0$. To obtain the poly(ST-*random*-MA) with various ST compositions, the ratio of ST and MA was varied. The molar composition and the molecular weight of the poly(ST-*random*-MA) were determined by the NMR and the GPC calibrated with PS standards, respectively. The molecular characteristics of the poly(ST-*random*-MA) are listed in Table 3. The spin-label was carried out via ester−amide interchange reaction between the incorporated *tert*-butyl moieties in the poly(ST-*random*-MA) and 4-amino-TEMPO.

7. PS Homopolymers (1 and 2 in Figure 1). PS homopolymers were selectively spin-labeled at the chain end (1 in Figure 1) or the inside (2 in Figure 1) of the chain. The selective spin-label for the PS homopolymer has been described previously.[32]

8. Chain End of PMA Homopolymer (8 in Figure 1). PMA was polymerized at 368 K via the ATRP with the CuBr/PMDETA complex and 2-BABE as an initiator.[39] After the polymerization, the PMA was purified by the precipitation from toluene solution into excess methanol. The PMA was dried in a vacuum at 353 K for 24 h. 4-Amino-TEMPO was reacted with the incorporated *tert*-butyl moiety at the α end. The M_n and M_w/M_n of the PMA were determined by the GPC calibrated with PS standards.

9. Inside of PMA Homopolymer (9 in Figure 1). PMA which was randomly containing a few molar percent of *t*BA was obtained by the random copolymerization of MA and *t*BA via the ATRP with the CuBr/PMDETA complex and MBrP as an initiator. The copolymerization was carried out with the following condition: $[MA]_0 = 99[tBA]_0$, $[MBrP]_0 = 2[CuBr]_0 = 2[PMDETA]_0$, $[MA]_0 = 350[MBrP]_0$. The *tert*-butyl moieties randomly incorporated into the inside of the PMA chain were reacted with 4-amino-TEMPO.

10. Junction Point of PS-*block*-PEA (11 in Figure 8). PS-*block*-PEA spin-labeled at the junction point was prepared by completely the same procedure with the PS-*block*-PMA labeled at the junction point using EA instead of MA.

11. Inside of Poly(ST-*random*-EA) (13 in Figure 8). Poly(ST-*random*-EA) spin-labeled at the inside of the chain was prepared by completely the same procedure with the poly(ST-*random*-MA) labeled at the inside of the chain using EA instead of MA. The molar composition and the molecular weight of the poly(ST-*random*-EA) were determined by the NMR and the GPC calibrated with PS standards.

12. Inside of PEA (12 in Figure 8). PEA which was randomly containing a few molar percent of *t*BA was synthesized by the random copolymerization of EA and *t*BA via the ATRP with the CuBr/PMDETA complex and MBrP as an initiator. After the copolymerization, the spin-label and the purification were carried out with completely the same procedure with the PMA labeled at the inside of the chain. The

M_n and M_w/M_n of the PEA were determined by the GPC calibrated with PS standards.

Film Preparation. The spin-labeled PS-*block*-PMA, poly(ST-*random*-MA), PS-*block*-PEA, poly(ST-*random*-EA), and the PS, PMA, and PEA homopolymers were dissolved into toluene at 5 wt %. These solutions were dried slowly at a room temperature on a Teflon plate. After the films were dried (for a week), the PS-*block*-PMA, poly(ST-*random*-MA), PS-*block*-PEA, poly(ST-*random*-EA), and PS films were annealed in a vacuum at 393 K for 24 h. The PMA and PEA films were annealed in a vacuum at 353 K for 24 h.

Measurements. Small-angle X-ray scattering (SAXS) measurement was performed at beamline BL-9C and 15A in Photon Factory (PF) of the High Energy Accelerator Research Organization (KEK) in Tsukuba, Japan. White radiation from the source was monochromatized using a double monochromator of Si(111) crystal to give an intense beam of $\lambda = 0.1499$ nm X-rays. The detector is one-dimensional position-sensitive proportional counters (PSPC) located at a distance of 1.0 m (BL-9C) and 2.3 m (BL-15A) from the sample position. Collagen (chicken tendon) was used as a standard specimen to calibrate the SAXS detector. The experimental data were corrected for the background scattering and sample absorption.

The NMR was performed on a Bruker AVANCE 200 spectrometer using deuterated chloroform as a solvent at 298 K with tetramethylsilane as an internal reference.

The M_n and M_w/M_n of samples were determined by the GPC in THF (1 mL/min) at 313 K on four polystyrene gel columns (Tosoh TSK gel GMH (beads size is 7 μm), G4000H, G2000H, and G1000H (5 μm)) that were connected to a Tosoh CCPE (Tosoh) pump and an ERC-7522 RI refractive index detector (ERMA Inc.). The columns were calibrated against standard polystyrene (Tosoh) samples.

The each sample was contained in a quartz tube and the tube was depressurized to a pressure of 10^{-4} Torr and sealed before ESR measurement. ESR spectra at 77 K and higher temperatures were observed at low microwave power level to avoid power saturation and with 100 kHz fielded modulation using JEOL JES-FE3XG and JES-RE1XG spectrometers (X band) coupled to microcomputers (NEC PC-9801). The signal of 1,1-diphenyl-2-picrylhydrazyl (DPPH) was used as a g tensor standard. The magnetic field was calibrated with the well-known splitting constants of Mn^{2+}.

A modulated-temperature differential scanning calorimetry (MDSC, MDSC 2920) manufactured by TA Instruments was used. A modulation amplitude of 1.5 K and a period of 60 s were used at a heating rate of 2 K/min. The calorimeter was calibrated with an indium standard.

Results and Discussion

1. Morphology of PS-*block*-PMA. The SAXS was utilized to determine the morphology of the PS-*block*-PMA and PS-*block*-PEA. SAXS profiles for the PS-*block*-PMA ($M_n = 42.2$K, $M_w/M_n = 1.15$, $M_{n,PS} = 27$K, $\phi_{PMA} = 0.43$) in the temperature range 293−473 K are shown in Figure 2. The q_n/q^* ratio of 1, 2, 3, and 4 indicates a lamellar morphology. Here, q^* is the scattering vector of a primary scattering peak and q_n is the series of all scattering vectors for which peaks are observed. The lamellar morphology was observed for all PS-*block*-PMA's and PS-*block*-PEA used in this work at a room temperature. From the SAXS data, the lamellar domain spacing of the PS-*block*-PMA was found to be 39.8 ± 0.5 nm at 293 K. Although the lamellar spacing increased to be 41.8 ± 0.5 nm at 473 K due to the thermal expansion of the PS-*block*-PMA, the peaks did not diminish and higher-order peaks remained. This result demonstrated that morphological transitions did not occur for this PS-*block*-PMA in this temperature range. MDSC data also supported the microphase-separation of the PS-*block*-PMA. The MDSC curve of the PS-*block*-PMA exhibited two distinct steps, indicating the microphase separation (see Figure 6).

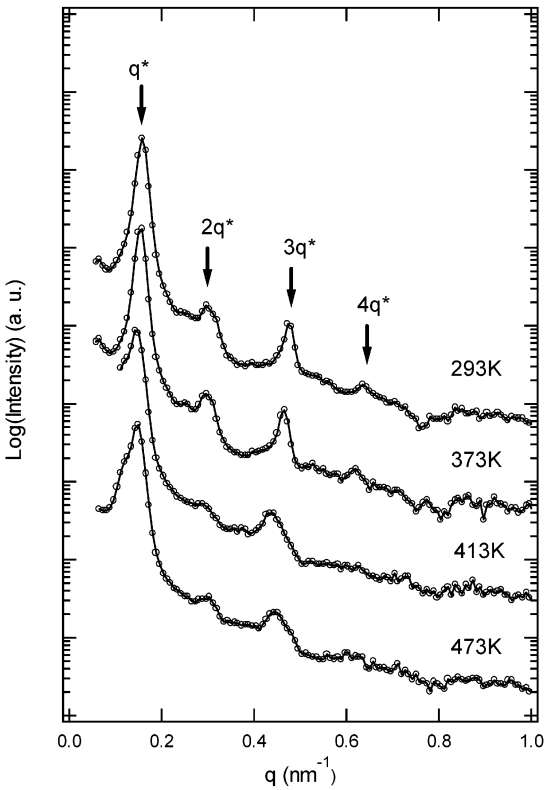

Figure 2. Plot of temperature-dependent log(I) vs q SAXS data of PS-*block*-PMA.

2. Molecular Motion in the Specific Sites of PS-*block*-PMA. 2.1. The Broad Distribution of Correlation Time for PS-*block*-PMA. Temperature-dependent ESR spectra of the PS homopolymer labeled at the inside of the chain (no. 2 in Table 1) with that of the PS-*block*-PMA labeled at the inside of the PS block (no. 4 in Table 1) in the temperature range 77−453 K were compared (Figure 3). The temperature dependence of the line shape of ESR spectra is due to the change in the motional correlation time, τ_c. The outermost splitting width of the main triplet spectrum due to hyperfine coupling caused by the nitrogen nucleus narrows with an increase in mobility of the radicals because of motional averaging of the anisotropic interaction between an electron and a nucleus. The complete averaging gives rise to the isotropic narrowed spectrum. Two spectral components, a "fast" and a "slow" component, are observed in the temperature-dependent ESR spectra of the PS-*block*-PMA labeled at the inside of the PS block. In general, the two spectral components are observed in a certain temperature range for crystalline polymers, polymer blends, block and graft copolymers, etc.[20,21,31,40−44] The slow component with the large outermost splitting width and the fast component with small outermost splitting width and narrow line width can be attributed to radicals in rigid and mobile regions, respectively. This is a reflection of a broad distribution of the τ_c arising from a heterogeneous structure of the PS block chain in the microdomain. For example, the heterogeneity of the segmental density or the free volume affected by the mobile PMA phase can originate the distribution of the τ_c. In contrast with the PS-*block*-PMA, the single component was observed for the PS homopolymer labeled at the inside of the chain.

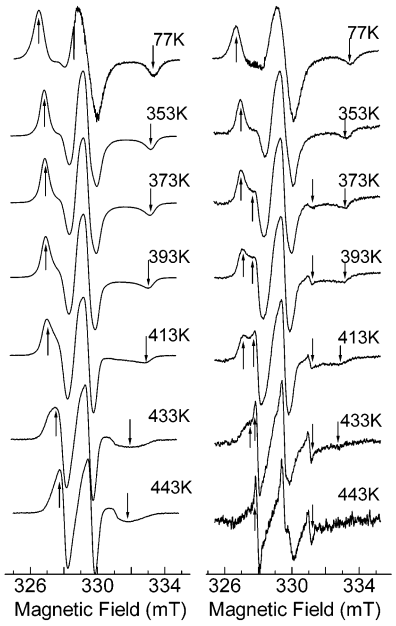

Figure 3. Temperature-dependent ESR spectra of PS homopolymer labeled at inside of chain (left) and PS-*block*-PMA labeled at inside of PS block (right). The separation between arrows shows the extreme separation width.

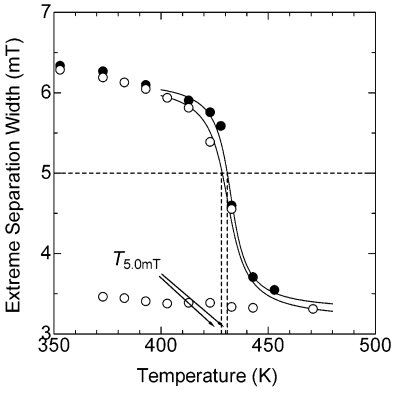

Figure 4. Temperature dependence of extreme separation width for PS labeled at inside (solid) and PS-*block*-PMA labeled at inside of PS block (open).

2.2. Comparison of Molecular Mobility of the PS Block in PS-*block*-PMA with That of PS Homopolymer. The extreme separation width between arrows shown in Figure 3 gradually narrows and steeply drops with an increase in temperature. The temperature dependence of the extreme separation width for each specimen is shown in Figure 4. The steep drop is caused by a micro-Brownian type molecular motion.[45−47] We estimated the transition temperature of the molecular motion, $T_{5.0mT}$, at which the extreme separation width is equal to 5.0 mT. The $T_{5.0mT}$ of the PS homopolymer labeled at the inside of the chain and that of the PS-*block*-PMA labeled at the inside of the PS block are 431 and 428 K, respectively. The $T_{5.0mT}$ includes ±2 K of experimental uncertainties. In general, the $T_{5.0mT}$ appears at higher than a glass transition temperature, T_g, obtained by DSC because of a higher frequency corresponding to the rate of averaging of the anisotropic hyperfine splitting.[45−47] Previously, we compared the $T_{5.0mT}$ with the T_g of the PS homopolymer in detail.[32] In the previous paper, the $T_{5.0mT}$ was reduced to a transition temperature, $T_{g,ESR}$, for $\tau = 100$ s[48,49] by the WLF equation.[50] The $T_{g,ESR}$ agreed well with the T_g obtained by the MDSC. This result demonstrates that the $T_{5.0mT}$ reflects the glass transition. The $T_{5.0mT}$ of the PS block is slightly lower than the $T_{5.0mT}$ of the PS homopolymer because of premature molecular motion of the PS block induced by the mobile PMA phase. In particular, the fast component with the small outmost splitting mentioned above was attributed to the PS segment located near the mobile PMA phase. Wardell et al. studied the molecular motion of the PS chain in the microphases of polystyrene-*block*-polybutadiene-*block*-polystyrene (SBS) triblock copolymer using broadband proton pulsed NMR.[17,18] They reported that the T_g of the PS microdomain was lower than that of the PS homopolymer. They interpreted the behavior in terms of premature molecular motions of the PS block chains in the PS microdomain induced by the highly mobile chains in the PB phase.

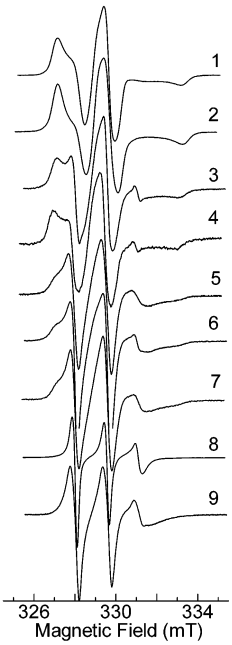

Figure 5. Comparison of ESR spectra of spin-labeled PS-*block*-PMA, and PS and PMA homopolymers at various sites of chain observed at 393 K. Numbers of spectra correspond to numbers in Figure 1.

2.3. Molecular Motion of Specific Sites of PS-*block*-PMA. ESR spectra of the selective spin-labeled PS and PMA homopolymers and the PS-*block*-PMA's (1−9 in Figure 1) observed at 393 K are shown in Figure 5 to compare with each other. It was found that the molecular mobility strongly depends on the local environments. For the PMA homopolymer, phase matching is very difficult at high temperatures because of a polar fluid of PMA which is resulting in absorbing the energy of the microwave strongly. As a result, the dephased spectra (8 and 9 in Figure 5) were observed with the fairy different peak height on and under the zero level. The $T_{5.0mT}$'s of the samples are shown in Table 1. The PS-*block*-PMA's spin-labeled at five specific sites showed different $T_{5.0mT}$'s. The molecular mobility at 393 K and the transition temperatures have an order of 4 > 3 > 5 > 6 > 7. The molecular mobilities of the PS and PMA block ends were respectively higher than those of the inside of the PS and PMA blocks due to the large specific free volume around the chain ends. The molecular mobility changes from the low mobility in the PS block to the high one in the PMA block in order along a chain of the PS-*block*-PMA. The two spectral components were

not observed for all homopolymers (Table 1). This result demonstrates that the distribution of the free volume or the segmental density is narrow on the spin-labeled sites of the homopolymers. On the other hand, the two spectral components were observed for all PS-*block*-PMA's spin-labeled at various sites of the chain. The two spectral components imply the broad distribution of the free volume or the segmental density in the microdomains of the PS-*block*-PMA. It was considered that the differences of the molecular mobility of the PS-*block*-PMA's at the specific sites were arisen from the heterogeneity of the local structure and the local environment in the lamellar microdomains. In contrast with the PS block, the $T_{5.0mT}$ of the PMA block labeled at the inside was higher than that of the PMA homopolymer labeled at the inside of the chain because the rigid PS phase restricted the molecular motion of the mobile PMA block chains. The elevated T_g of the soft component of the microphase-separated block copolymer in comparison with the homopolymer has been frequently reported.[3,8−12]

2.4. Molecular Motion of the Chain Ends of PS and PMA Blocks in PS-*block*-PMA. The $T_{5.0mT}$'s of the PS and PMA homopolymers and the PS-*block*-PMA labeled at their chain ends were lower than those of the ones labeled at the inside of their chains because of the relatively large free volume around the chain end to that of other sites. Recently, we reported that the chain end has a lower transition temperature than that of the inside segment of PS at the glass transition due to the large specific free volume around the chain end.[32] The differences between the $T_{5.0mT}$'s of the PS and PMA homopolymers labeled at the chain end and those at the inside of the chain were 8 and 4 K, respectively. On the other hand, the difference between the $T_{5.0mT}$ of the PS-*block*-PMA labeled at the chain end and that at the inside of the PS block was 14 K. Similarly, the difference for the PMA block was 15 K. These differences for the PS-*block*-PMA were significantly larger than those for the PS and PMA homopolymers. The much higher molecular mobility of the chain ends of the PS-*block*-PMA is considered to be caused by the chain conformation of the PS-*block*-PMA chains in the lamellar microdomains. In our previous paper, we detected that the molecular mobility of the chain end of the PS homopolymer increased with a decrease in the molecular weight, and the increase was brought by the local large free volume around the chain end induced by an encounter of more than two chain ends.[32] The remarkably enhanced molecular mobility of the chain ends of the PS-*block*-PMA is also interpreted in terms of the local large free volume around the chain end induced by the local high concentration of the chain ends in the lamellar microdomains. SANS measurements by Russell et al. and Matsushita et al. revealed that chain ends of diblock copolymers were concentrated on the center of the lamellar microdomains with a fairly wide distribution.[33−35] The concentration of the chain ends implies an increase in the probability of the encounter of chain ends. As a result, the much large free volume is formed around the chain ends of the PS-*block*-PMA in the lamellar microdomains, which enhances the molecular mobility of the chain ends of the PS-*block*-PMA.

3. Interfacial Region of Microdomains. Much interest has been directed toward the nature of the microdomain interface. In particular, the molecular mobility of the interfacial region is important for understanding the mechanical property of incompatible polymer alloys. Unfortunately, experimental measurements of the microdomain interface are difficult because of its extremely small dimension and the interface is a region of undefined composition. For example, an incompatible diblock copolymer generally exhibits only two distinct steps induced by the glass transitions of the microphase-separated components in a DSC curve (see Figure 6). Although one cannot find the step brought from the glass transition of the interfacial region, the losses of the increment of heat capacities associated at the glass transitions of the each component are observed (see Table 2). This loss of the increment of the heat capacity implies the existence of the interfacial region of the microphase-separated domains.[3] The glass transition of the interfacial region is considered to exist over a wide range of temperature between the glass transitions of the each component of the diblock copolymer because the composition of the interfacial region is not defined well. The chemical junction points of the diblock copolymers are concentrated in the interfacial region of microphase-separated domains.[33−35,51−54] We expect that the molecular mobility of the PS-*block*-PMA labeled at the junction point reflects the local environment of the interfacial region of the microdomains because of the strong localization of the junction points on the interfacial region. The $T_{5.0mT}$ of the PS-*block*-PMA labeled at the junction point (398 K) was roughly intermediate between those of the PS-*block*-PMA labeled at the inside of the PS block (428 K) and the PMA block (395 K). This fact suggests that the PS and PMA chains are mixed at a molecular level in the interfacial region. Dowrey et al. studied the molecular mobility of the interfacial region of the microphase-separated structure of polystyrene-*block*-polyisoprene (PS-*block*-PI) using dynamic infrared linear dichroism spectroscopy.[51] They reported that the styrene segment near the junction point lied in the interfacial region and had rubberlike mobility even at a room temperature. Our result agrees well with their result. The interfacial region has higher molecular mobility than that of the rigid PS phase owing to the effect of the mobile PMA phase. It has represented that the both components of the incompatible diblock copolymer are mixing with a gradient of the segmental concentration in the interfacial region of microdomains.[52] The thickness of the interfacial region has been also determined by some experiments[3,52−56] and theories.[57−59]

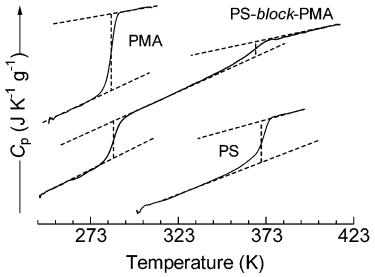

Figure 6. MDSC curves of PS-*block*-PMA (no. 5 in Table 1) and PS (no. 2 in Table 1) and PMA (no. 9 in Table 1) homopolymers at 2 K/min with modulation amplitude of 1.5 K and 60 s period.

3.1. Estimation of the Interfacial Thickness. The MDSC curve of the PS-*block*-PMA (no. 5 in Table 1) was compared to that of the PS (no. 2 in Table 1) and PMA (no. 9 in Table 1) homopolymers in Figure 6. The PS-

block-PMA exhibits two distinct steps in the MDSC curve, indicating the microphase separation. One can estimate the increase in the heat capacity, ΔC_p, associated at the glass transitions of the PS and PMA phases. The ΔC_p's of each phase in the PS-*block*-PMA are evaluated from the difference in the height between the extrapolated baselines recorded before and after the transition, the temperature at which corresponds to the half-height of the baseline shift. This is illustrated by the broken lines in Figure 6. The same temperature is arbitrarily chosen for characterizing the T_g's of each phase. The values of $T_{g,1}$ and $\Delta C_{p,1}$ associated with the PMA phase, together with those of $T_{g,2}$ and $\Delta C_{p,2}$ associated with the PS phase are listed in Table 2. The $T_{g,\,PS}$ and $\Delta C_{p,PS}$ were evaluated for the PS homopolymer, the $T_{g,PMA}$ and $\Delta C_{p,PMA}$ were evaluated for the PMA homopolymer (Table 2). For comparison, the values of the ΔC_p per gram were evaluated for each phase (PS or PMA) in the material. The $T_{g,1}$ and $T_{g,2}$ were higher and lower than the $T_{g,PMA}$ and $T_{g,PS}$, respectively. This result corresponded to the result of the estimation of the molecular mobility at the specific sites of the PS-*block*-PMA by the ESR measurements. As mentioned above, the $T_{5.0mT}$'s of the PS-*block*-PMA's labeled at the inside of the PS and PMA blocks were also lower and higher than those of the PS and PMA homopolymers labeled at the inside of the chains, respectively (Table 1).

The losses of the ΔC_p's at the two distinct transitions of the PS-*block*-PMA are observed, and the loss is considered to be caused by the existence of the mixed interfacial region of the microdomains. The glass transition of the mixed interfacial region is considered to exist over a wide range of temperature between the $T_{g,1}$ and $T_{g,2}$ because the undefined composition of the interfacial region. On the basis of this idea, Morèse-Séguéla et al. derived the following equation[3] to determine the thickness of the interfacial region of the lamellar microdomains of the PS-*block*-PI using DSC.

$$t_i = (t_s/2)[1 - (\Delta C_{p,2}/\Delta C_{p,PS})] \qquad (1)$$

Here, t_i and t_s are the thickness of the interfacial region and the PS lamellar domain, respectively. $\Delta C_{p,PS}$ is the increment of the heat capacity at the glass transition of the PS homopolymer. The value of the t_s was calculated to be 19 nm from the lamellar domain spacing determined by the SAXS measurement and the volume fraction of the PS component. The t_i of the PS-*block*-PMA (no. 5 in Tables 1and 2) was calculated to be 1.6 nm.

3.2. Molecular Motion of the Junction Point of PS and PMA Blocks in the Interfacial Region. Some authors pointed out that the characteristics of an interfacial region of an incompatible block copolymer are assumed to be that of the random copolymer of the both components.[57−59] Therefore, the comparison of the molecular mobility of the PS-*block*-PMA labeled at the junction point with that of the spin-labeled poly(ST-*random*-MA) should be valuable for considering the structure and environment of the interfacial region. The poly(ST-*random*-MA)'s labeled at the inside of the chain with various ST compositions were prepared. Important molecular characteristics of the poly(ST-*random*-MA) are listed in Table 3. The $T_{5.0mT}$'s of the spin-labeled poly(ST-*random*-MA) and those the PS and PMA homopolymers labeled at the inside of the chain are plotted as a function of the ST weight fraction in Figure 7. The ESR spectra of the poly(ST-*random*-MA) labeled at the inside of the chain with various ST weight fractions observed at 413 K are also exhibited in Figure 7. In general, the T_g of the random copolymer lies between the T_g's of the respective homopolymers depending on their composition. The Gordon−Taylor equation is the most basic to expect the T_g of random copolymers.[60] The Gordon−Taylor equation is given by

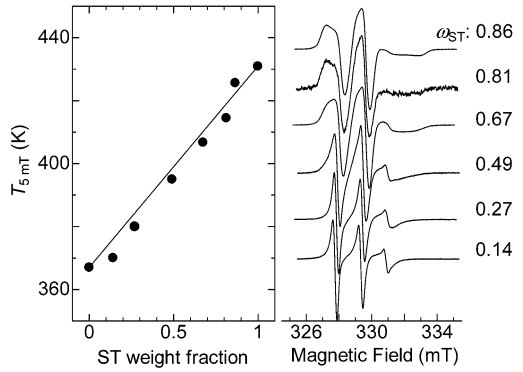

Figure 7. Plot of $T_{5.0mT}$ of spin-labeled PS, PMA, and poly(ST-*random*-MA) as a function of ST weight fraction (ω_{PS}). The solid line is presented by the Gordon−Taylor equation. Comparison of ESR spectra of spin-labeled poly(ST-*random*-MA) with various ST compositions observed at 413 K.

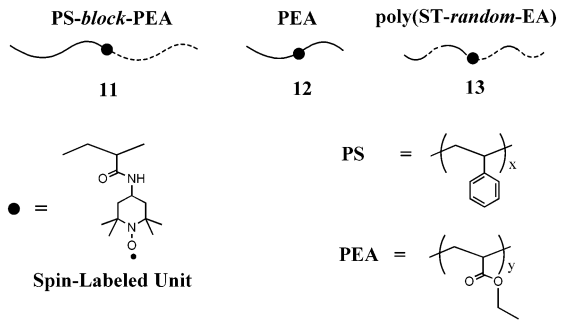

Figure 8. Chemical structures and illustrations of selectively spin-labeled PS-*block*-PEA, poly(ST-*random*-EA), and PEA homopolymer.

$$T_g = (T_{gA}w_A + KT_{gB}w_B)/(w_A + Kw_B) \qquad (2)$$

where w_A and w_B are weight fractions of each component and T_{gA} and T_{gB} are the T_g of the respective homopolymers. Here, the parameter K is assumed to be unity for simplicity. Rieger et al. reported that the T_g of the poly(ST-*random*-MA) agreed well with the Gordon−Taylor equation.[61] The $T_{5.0mT}$ which is detected at higher frequency should also follow the Gordon−Taylor equation. In the case of the ST weight fraction of 0.5, the $T_{5.0mT}$ of the poly(ST-*random*-MA) was interpolated to be 399 K by the Gordon−Taylor relation, which was in good agreement with the $T_{5.0mT}$ of the PS-*block*-PMA labeled at the junction point (398 K) within experimental uncertainties. The $T_{5.0mT}$ of PS-*block*-PEA labeled at the junction point also nearly equaled to the $T_{5.0mT}$ of poly(ST-*random*-EA) labeled at the inside of the chain with the ST weight fraction of 0.5. Important characteristics and molecular structures of the PS-*block*-PEA, poly(ST-*random*-EA), and PEA homopolymer are shown in Table 3 and Figure 8. The lamellar morphology of the PS-*block*-PEA was also determined by the SAXS measurement at a room temperature. Temperature-dependent ESR spectra of the PS-*block*-PEA labeled at the junction point are shown in Figure 9. The spectra exhibited the two spectral components and the $T_{5.0mT}$

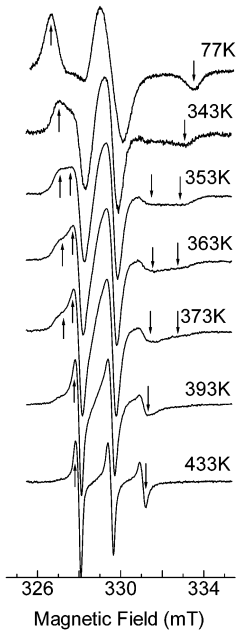

Figure 9. Temperature-dependent ESR spectra of PS-*block*-PEA labeled at junction point. The separation between arrows shows the extreme separation width.

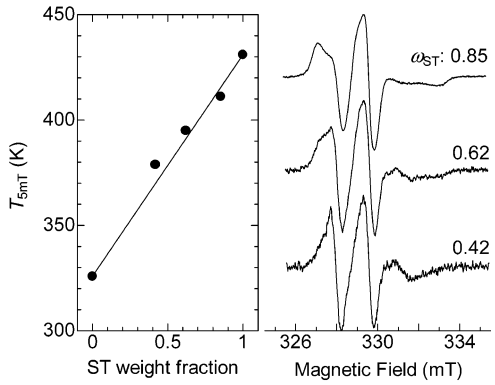

Figure 10. Plot of $T_{5.0mT}$ of spin-labeled PS, PEA, and poly(ST-*random*-EA) against ST weight fraction (ω_{PS}). The solid line is presented by the Gordon−Taylor equation. Comparison of ESR spectra of spin-labeled poly(ST-*random*-EA) with various ST compositions observed at 393 K.

of the PS-*block*-PEA labeled at the junction point was determined to be 379 K. The $T_{5.0mT}$ of the poly(ST-*random*-EA) labeled at the inside of the chain was plotted against the ST weight fraction in Figure 10. The ESR spectra of the poly(ST-*random*-EA) labeled at the inside of the chain with various ST weight fractions observed at 393 K are also shown in Figure 10. In the case of the ST weight fraction of 0.5, the $T_{5.0mT}$ of the poly(ST-*random*-EA) was interpolated to be 379 K by the Gordon−Taylor relation. The $T_{5.0mT}$ of the PS-*block*-PEA labeled at the junction point also almost coincided with that of the poly(ST-*random*-EA) labeled at the inside of the chain with the ST weight fraction of 0.5. Moreover, asymmetrical PS-*block*-PMA's labeled at the junction point were synthesized (M_n = 40.2K, M_w/M_n = 1.14, $M_{n,PS}$ = 30K, and ϕ_{PMA} = 0.30; M_n = 65.1K, M_w/M_n = 1.46, $M_{n,PS}$ = 30K, and ϕ_{PMA} = 0.56). Even though these PS-*block*-PMA's had different molecular weights and compositions, the $T_{5.0mT}$'s of these PS-*block*-PMA's corresponded to be 398 K within experimental errors. These results support that the both components of diblock copolymers are compatibly mixing with each other in the interfacial region. The thermal behavior of the junction points of the diblock copolymers in the interfacial region roughly agreed with that of the random copolymer, and we suggest that the thermal behavior of the interfacial region can be expected to be that of the random copolymer roughly. However, fundamental differences between the random copolymer and the interfacial region should be discussed. Although the $T_{5.0mT}$ of the interfacial region corresponded to that of the random copolymer with the ST weight fraction of 0.5 within experimental errors, the perfect characterization of the interfacial region might be hard from only our ESR results. The remarkably different point is two spectral components observed in the temperature-dependent ESR spectra of diblock copolymers labeled at the junction point in contrast to the single spectral component in those of the homopolymers and random copolymers. The two spectral components of the block copolymers labeled at the junction points are considered to be caused by the heterogeneous structure (concentration heterogeneity of the each segment) around the spin-labels in the interfacial region. Here, two characteristic temperatures, T_f and T_s, were estimated for the PS-*block*-PMA and PS-*block*-PEA labeled at the junction point. The T_f is where the sharp ^{14}N isotropic triplet spectrum appears as the sample is warmed, while the T_s is where the broad spectrum identified with the anisotropic pattern disappears. The method for determination of the T_f and T_s was described in detail in our previous paper.[61] The T_f's of the PS-*block*-PMA (363 ± 3 K) and PS-*block*-PEA (330 ± 3 K) are nearly equal to the $T_{5.0mT}$'s of the PMA (367 K) and PEA (326 K) homopolymers, respectively, and the T_s's of the PS-*block*-PMA (437 ± 5 K) and PS-*block*-PEA (427 ± 5 K) are roughly agreed with the $T_{5.0mT}$ of the PS homopolymer (431 K). This suggests that the spin-labels are distributed in the interfacial region, and some of the spin-labels are located near the each domain. The molecular mobility of the junction point obtained by the ESR measurements strongly reflected the environmental features of the interfacial region.

Conclusion

The molecular motion at the specific sites of the PS and PMA homopolymers and the PS-*block*-PMA forming the lamellar microphase-separated structure were determined by the ESR selective spin-label method. The molecular motion reflected the local environmental features of the spin-labeled sites. It was revealed that the molecular mobility of the chain end was higher than that of the inside sites for the PS-*block*-PMA and the PS and PMA homopolymers because of the relatively large free volume around the chain end to those of other sites. Moreover, the enhanced molecular mobility of the both chain ends of the PS-*block*-PMA forming the lamellar morphology was more remarkable than those of the both homopolymers. This remarkable enhancement is considered to be brought from the much large free volume around the chain ends because of the concentration of the chain ends induced by the localization of the junction point at the interface in the lamellar microdomains. The perpendicular extension of the block chains to the interface and the concentration of the chain ends of the diblock copolymers at the center of the lamellar microdomains were revealed by Russell et al. and Matsushita et al. using SANS. The molecular motion of the PS-*block*-PMA labeled at the junction point reflected the characteristics of the interfacial

region of the lamellar microdomains due to the strong localization of the junction point in the interfacial region. The thickness of the interfacial region of the PS-*block*-PMA was estimated to be 1.6 nm by the combination of the SAXS and MDSC measurements. The transition temperature, $T_{5.0mT}$, of the PS-*block*-PMA labeled at the junction point (398 K) roughly agreed with that of the poly(ST-*random*-MA) with the ST weight fraction of 0.5 (399 K) interpolated by the Gordon−Taylor relation. Moreover, the $T_{5.0mT}$ of the PS-*block*-PEA labeled at the junction point (379 K) was also nearly equal to that of the poly(ST-*random*-EA) labeled at the inside of the chain with the ST weight fraction of 0.5 (379 K) interpolated by the Gordon−Taylor relation. The two spectral components of the temperature-dependent ESR spectra of the PS-*block*-PMA and PS-*block*-PEA labeled at the junction points are brought from the broad distribution of the τ_c, and it indicates the heterogeneous structure in the interfacial region. These results are considered to reflect the structural and environmental features of the interfacial region; i.e., the both components of the diblock copolymers are mixing in a molecular level heterogeneously. In conclusion, the ESR selective spin-label method is the advantageous and informative method to reveal the molecular motion and the local environment at the specific sites of diblock copolymers forming the microphase-separated structure.

Acknowledgment. Thanks are due to the Research Center for Molecular-Scale Nanoscience, the Institute for Molecular Science, for assistance in obtaining the MDSC data. The SAXS measurement was performed under approval of the Photon Factory Program Advisory Committee (Proposal No. 2001G269 and 2001G275). The financial support of a part of this project is by a grant from the NITECH 21st Century COE Program "World Ceramics Center for Environmental Harmony".

References and Notes

(1) Hamley, I. W. *The Physics of Block Copolymers*; Oxford University Press: Oxford, England, 1998.
(2) Utracki, L. A. *Polymer Alloys and Blends*: *Thermodynamics and Rheology*; Hanser Publishers: Munich, 1990.
(3) Morèse-Séguéla, B.; St-Jacques, M.; Renaud, J. M.; Prud'homme, J. *Macromolecules* **1980**, *13*, 100.
(4) Krause, S.; Iskandar, M.; Iqbal, M. *Macromolecules* **1982**, *15*, 105.
(5) Krause, S.; Iskandar, M. *Adv. Chem. Ser.* **1979**, *176*, 205.
(6) Gaur, U.; Wunderlich, B. *Macromolecules* **1980**, *13*, 1618.
(7) Toporowski, P. M.; Roovers, J. E. L. *J. Polym. Sci., Polym. Chem. Ed.* **1976**, *14*, 2233.
(8) Kraus, G.; Rollmann, K. W. *J. Polym. Sci., Polym. Phys. Ed.* **1976**, *14*, 1133.
(9) Mohammady, S. Z.; Mansour, A. A.; Knoll, K.; Stoll, B. *Polymer* **2002**, *43*, 2467.
(10) Kraus, G.; Childers, C. W.; Gruver, J. T. *J. Appl. Polym. Sci.* **1967**, *11*, 1581.
(11) Cowie, J. M. G.; Lath, D.; McEwen, I. J. *Macromolecules* **1979**, *12*, 52.
(12) Cowie, J. M. G.; McEwen, I. J. *Macromolecules* **1979**, *12*, 56.
(13) Enns, J. B.; Rogers, C. E.; Simha, R. *Adv. Chem. Ser.* **1979**, *176*, 217.
(14) Lu, Z.; Krause, S. *Macromolecules* **1982**, *15*, 112.
(15) Dollase, T.; Graf, R.; Heuer, A.; Spiess, H. W. *Macromolecules* **2001**, *34*, 298.
(16) Rittig, F.; Kärger, J.; Paparakis, C. M.; Fleischer, G.; Almdal, K.; Štěpánek, P. *Macromolecules* **2001**, *34*, 868.
(17) Wardell, G. E.; McBrierty, V. J.; Douglass, D. C. *J. Appl. Phys.* **1974**, *45*, 3341.
(18) Bianchi, U.; Pedemonte, E.; Turturro, A. *Polymer* **1970**, *11*, 268.
(19) Kumler, P. L.; Keinath, S. E.; Boyer, R. F. *Polym. Eng. Sci.* **1977**, *17*, 613.
(20) Cameron, G.; Qureshi, M. Y.; Tavern, S. C. *Eur. Polym. J.* **1996**, *32*, 587.
(21) Brown, I. M. *Macromolecules* **1981**, *14*, 801.
(22) Varghese, B.; Schlick, S. *J. Polym. Sci., Part B: Polym. Phys.* **2002**, *40*, 424.
(23) Shimada, S.; Hori, Y.; Kashiwabara, H. *Macromolecules* **1985**, *18*, 170.
(24) Hori, Y.; Makino, Y.; Kashiwabara, H. *Polymer* **1984**, *25*, 1436.
(25) Shimada, S.; Hori, Y.; Kashiwabara, H. *Macromolecules* **1988**, *21*, 979.
(26) Shimada, S.; Watanabe, T. *Polymer* **1998**, *39*, 1703.
(27) Shimada, S.; Horiguchi, K.; Yamamoto, K. *Colloid Polym. Sci.* **1998**, *276*, 412.
(28) Shimada, S.; Sugimoto, A.; Kawaguchi, M. *Polymer* **1997**, *38*, 2251.
(29) Shimada, S.; Watanabe, T. *Polymer* **1998**, *39*, 1711.
(30) Shimada, S.; Hane, Y.; Watanabe, T. *Polymer* **1997**, *38*, 4667.
(31) Schlick, S.; Harvey, R. D.; Alonso-Amigo, M. G.; Klempner, D. *Macromolecules* **1989**, *22*, 822.
(32) Miwa, Y.; Tanase, T.; Yamamoto, K.; Sakaguchi, M.; Sakai, M.; Shimada, S. *Macromolecules* **2003**, *36*, 3235.
(33) Mayes, A. M.; Johnson, R. D.; Russell, T. P.; Smith, S. D.; Satija, S. K.; Majkrzak, C. F. *Macromolecules* **1993**, *26*, 1047.
(34) Torikai, N.; Matsushita, Y.; Noda, I.; Karim, A.; Satija, S. K.; Han, C. C. *Physica B* **1995**, *213−214*, 694.
(35) Torikai, N.; Noda, I.; Karim, A.; Satija, S. K.; Han, C. C.; Matsushita, Y.; Kawakatsu, T. *Macromolecules* **1997**, *30*, 2907.
(36) Patten, T. E.; Xia, J.; Abernathy, T.; Matyjaszewski, K. *Science* **1996**, *272*, 866.
(37) Matyjaszewski, K.; Patten, T. E.; Xia, J. *J. Am. Chem. Soc.* **1997**, *119*, 674.
(38) Ziegler, M. J.; Matyjaszewski, K. *Macromolecules* **2001**, *34*, 415.
(39) Davis, K. A.; Paik, H.; Matyjaszewski, K. *Macromolecules* **1999**, *32*, 1767.
(40) Shimada, S.; Kozakai, M.; Yamamoto, K. *Polymer* **1998**, *32*, 6013.
(41) Varghese, B.; Schlick, S. *J. Polym. Sci., Part B: Polym. Phys.* **2002**, *40*, 415.
(42) Cameron, G. G.; Qureshi, M. Y.; Stewart, D.; Buscall, R.; Nemcek, J. *Polymer* **1995**, *36*, 3071.
(43) Cameron, G. G.; Stewart, D. *Polymer* **1996**, *37*, 5329.
(44) Pannier, M.; Schöps, M.; Schädler, V.; Wiesner, U.; Jeschke, G.; Spiess, H. W. *Macromolecules* **2001**, *34*, 5555.
(45) Shimada, S.; Kashima, K. *Polym. J.* **1996**, *28*, 690.
(46) Sohma, J.; Sakaguchi, M. *Adv. Polym. Sci.* **1978**, *20*, 109.
(47) Kusumoto, N.; Sano, S.; Zaitsu, N.; Motozato, Y. *Polymer* **1976**, *17*, 448.
(48) Angell, C. A. *J. Non-Cryst. Solids* **1991**, *131−133*, 13.
(49) Ngai, K. L.; Plazek, D. J. *Rubber Chem. Technol.* **1995**, *68*, 376.
(50) Williams, M. L.; Landel, R. F.; Ferry, J. D. *J. Am. Chem. Soc.* **1995**, *77*, 3701.
(51) Smith, S. D.; Noda, I.; Marcott, C.; Dowrey, A. E. *Polymer Solutuins, Blends and Interfaces;* Elsevier Science Publishers*:* Amsterdam, 1992.
(52) Anastasiadis, S. H.; Russell, T. P.; Satija, S. K.; Majkrzak, C. F. *J. Chem. Phys.* **1990**, *92*, 5677.
(53) Ni, S.; Zhang, P.; Wang, Y.; Winnik, M. A. *Macromolecules* **1994**, *27*, 5742.
(54) Tcherkasskaya, O.; Ni, S.; Winnik, M. A. *Macromolecules* **1996**, *29*, 610.
(55) Rharbi, Y.; Winnik, M. A. *Macromolecules* **2001**, *34*, 5238.
(56) Hashimoto, T.; Todo, H.; Itoi, H. H. Kawai, H. *Macromolecules* **1977**, *10*, 377.
(57) Leary, D. F.; Williams, M. C. *J. Polym. Sci., Polym. Phys. Ed.* **1973**, *11*, 345.
(58) Meier, D. J. *Polym. Prepr. (Am. Chem. Soc., Div. Polym. Chem.)* **1974**, *15*, 171.
(59) Helfand, E. *Macromolecules* **1975**, *8*, 552.
(60) Gordon, M.; Taylor, S. J. *J. Appl. Chem.* **1952**, *2*, 4.
(61) Yamamoto, K.; Shimada, S.; Tsujita, Y.; Sakaguchi, M. *Macromolecules* **1997**, *30*, 1776.

MA035088Q